

Origin of Contrast Effects in the Electron Microscopy of Polymers

Part 1: *Polyethylene Single Crystals*

D. T. GRUBB, A. KELLER,

H. H. Wills Physics Laboratory, University of Bristol, Royal Fort, Tyndall Avenue, Bristol, UK

G. W. GROVES

Department of Metallurgy, University of Oxford, Oxford, UK

When polyethylene single crystals are mounted on a substrate less rigid than the usual evaporated carbon, they undergo considerable dimensional changes in the electron beam. In particular, crystals mounted on collodion expand by $22 \pm 2\%$ in every direction in the plane of the lamellae. No induction period is observed and the expansion continues after all crystalline order has been destroyed. Since irradiation increases the density of bulk polyethylene, it is presumed that the lamellae become thinner as they expand. A similar but lesser expansion occurs on irradiation in the electron microscope at liquid helium temperatures, and when crystals are mounted on formvar films.

In a solution grown lamellar crystal of polyethylene, most of each molecule is straight and aligned along the *c* axis, which is nearly perpendicular to the plane of the lamella. Radiation damage in the electron microscope introduces disorder, and these results imply that the effect of this disorder is to reduce the mean molecular dimension along *c*, and increase it in the plane perpendicular to *c*. Polymer chains are generally highly oriented in crystalline regions, so this qualitative explanation would imply similar effects in other systems. These effects have important implications for the contrast observed in the electron microscopy of polymers.

1. Introduction

From the first observations of polymer crystals in the electron microscope, it has been known that the electron beam used to image the specimen drastically affects the crystals. Until quite recently observation and study of the damaging effect of the beam has been confined to diffraction phenomena. Thus it was observed early in the work on polyethylene (PE) single crystals that the diffraction pattern of a crystal decays rapidly in the electron beam to a diffuse ring very like the diffraction pattern of amorphous carbons, and simultaneously all contrast effects due to Bragg diffraction disappear from the image [1]. This process is due to a combination of cross-linking and scission reactions (the former being prevalent in the much studied PE) which destroys the regularity of the crystal lattice. The process has been studied in detail

[2, 3] and has been used as a measure of the radiation damage of PE [4, 5]. At an intermediate stage the diffraction spots broaden and the 200 reflexions move inwards so that the pattern approaches hexagonal symmetry. Kobayashi and Sakaoku [4] commented that this increase in the *a* spacing was not accompanied by any change in the crystal dimensions. Kiho and Ingram [6] observed crystallographic phase changes in PE crystals deposited on evaporated carbon film on heating them above 90°C. They found the cause to be differential thermal expansion between the PE and the carbon film. This implies that the carbon film is a very effective constraint on any expansion of the crystal.

Most electron microscopy of polymers, however, has not been concerned with diffraction effects, but with the morphology as seen. Here

image detail is due to differences in mass contrast usually attributable to variation in sample thickness. The boundaries between the different regions, if distinct enough, are usually enhanced by conventional metal shadowing. In such purely morphological studies the diffracting power of the crystalline specimen has usually been destroyed by the beam long before the photographs are taken. This is a particularly common occurrence with biological specimens. It has always been tacitly assumed, without any guarantee, that apart from loss of diffraction contrast, the morphology observed is not affected. However, it has become gradually apparent that if self supporting films are viewed, significant contrast changes occur in the beam at doses well beyond those which destroy the diffraction patterns. Hence changes occur in specimens which have long ceased to diffract. We became particularly conscious of such changes when viewing PE spherulites either in the form of thin solvent cast films or as ultramicrotome sections cut from spherulitic bulk PE [7, 9]. Andrews [10] observed contrast changes in rubber spherulites and Harris [11] in a detailed study of spherulites of Nylon, deduced that the final contrast depended on crystallite orientation, regions with c axis parallel to the beam becoming lighter. The post-diffraction contrast changes were so pronounced in PE that it has become apparent that without an understanding of how and why they arise, interpretation of electron microscope images of continuous unstained films, including sections, will remain incomplete or even erroneous. The problem is particularly serious for the sections as it would preclude rational examinations of technological materials by transmission electron microscopy.

In order to attack this problem we reverted to the examination of PE single crystals in a form where they are less constrained by a substrate. Crystals mounted on a holey substrate showed that the stability of the normal preparation is conferred by the carbon film, as they crumpled in the beam. Measurement of changes in these crystals was very difficult; it was necessary to find a soft, flexible support. A starting point was an early observation reported in passing by Keller and Bassett [12]. It was stated (p. 255) that crystals deposited or embedded in nitrocellulose can appear brighter than their surrounding (fig. 21 of ref. 12. Compare crystal with darker bottom left corner of picture; at the time this picture area was not selected to illustrate this

particular effect at its best. This will be done in the present publication). Also it was noted at the time, even if not stated in ref. 12, that the greater transparency of the crystal compared with the nitrocellulose appeared to develop during observation, while in the beam. In the present study, it has been found that the nitrocellulose mounting gives the best demonstration of the behaviour of unconstrained crystals. As will be seen, the understanding gained in this way will be the foundation on which interpretation of post-diffraction contrast effects under more general conditions can be based.

2. Experimental Procedure

2.1. Specimen Preparation

Single crystals of PE were grown at 83°C from a 8.10^{-5} g/cc solution of Rigidex type 9 in xylene. The self seeding technique of Blundell *et al* [13] was used to give a homogeneous preparation of single crystals. A similar preparation made with Marlex 6009 as the starting material, and large single layer crystals of low molecular weight polymer grown at 84°C were used in some experiments.

Thin films of collodion were deposited on glass or mica from dilute solution in amyl acetate, the concentration controlling the thickness. PE crystals were deposited on the films by spraying a suspension onto them, and the films were then cut up and floated off on a water surface in the usual way. For some thick films, more collodion was deposited on top of the crystals so that they were within the film.

Some attempts were made to obtain crystals spanning holes on a grid without any continuous film support. For this purpose holey carbon film with sufficiently large holes was too delicate, and so a fine copper mesh was used. This mesh, kindly supplied by the English Electric Valve Co, had grid bars 7.5 microns wide, and square holes 9.2 microns across. Discs were punched from a sheet of this material and fitted in a specimen holder. Allowing a droplet of crystal suspension to evaporate on the grid, crystals are flattened by surface tension, and some bridge the holes in the mesh. If too much of the suspension is applied a mat begins to form.

2.2. Electron Microscopy

The electron microscope used was a Phillips EM 200 with goniometer stage operating at 80 or 100 kV. It was necessary to work rapidly at low magnifications and low beam currents. The beam

current density at the specimen, and thus the radiation dose, was measured with the exposure meter of the microscope, using a previously published calibration of collection efficiency [14] and an accurate magnification calibration.

3. Results

3.1. The Appearance and Expansion of PE Crystals

3.1.1. Crystals Mounted in Collodion

Figs. 1, 2 and 4-6 represent a selection of observations on the behaviour of collodion mounted crystals in the electron beam under a variety of mounting and irradiation conditions. The overall effect is immediately apparent:

- (1) the crystals become lighter compared with their surroundings;
- (2) the crystal area increases.

Fig. 1 shows a crystal mounted on a thin film

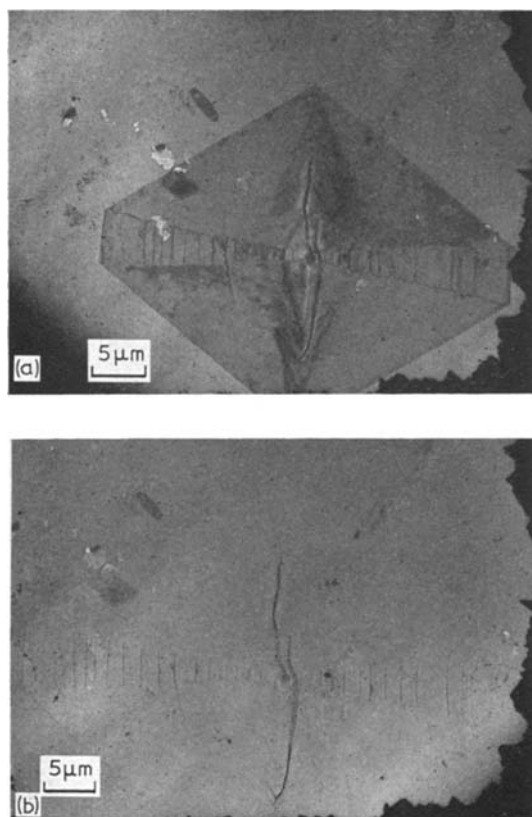


Figure 1 Single crystal of polyethylene mounted on a thin film of collodion. (a) Initial appearance in the electron microscope. (b) Final state after radiation damage by the imaging beam.

of collodion. The crystal can be seen clearly before there has been significant damage. In fig. 1a, taken after a radiation dose of 5 Coulombs/sq. metre at 80 kV, dark areas and streaks indicating crystalline diffraction contrast are visible, and even outside these areas the crystal is darker than its surroundings. In fig. 1b, taken after a dose of 500 Cm^{-2} without any adjustment to the microscope, the crystal has reversed contrast, and it has expanded considerably in its own plane. The angles of the crystal edges remain the same to within $\pm 1^\circ$, and by direct measurement the linear expansion is found to be the same in all directions in the plane, at $22 \pm 2\%$. The increase in lamellar area, measured by weighing photographic prints of several single layer crystals, is $53 \pm 7\%$. Taking the square root of this gives $24 \pm 3\%$ linear expansion, in good agreement with direct measurement. In fig. 1 the multilayer regions of the crystal, the central pleat and spiral overgrowths, remain darker than the rest of the crystal. The $\{100\}$ sectors are at places darker than the adjacent $\{110\}$ sectors in fig. 1b, but at other places they are lighter.

Fig. 2 again shows a PE single crystal mounted on collodion, but contains six pictures out of a sequence of twenty taken during the process of radiation damage. The first five, 2a-e, were given the same exposure and processing so that changes in transmitted intensity are shown correctly. The crystallographic diffraction contrast in fig. 2a has disappeared in fig. 2b, before the crystal reverses contrast, fig. 2c. In this period of radiation damage the diffraction spots gradually broaden. Subsequent pictures were taken after the diffuse arcs join up to form a ring, at 100 Cm^{-2} . From this sequence it is clear that the mass thickness of the collodion film is considerably reduced by irradiation. The mass loss of a PE film under similar conditions is only 5% [15]. The sixth picture, fig. 2f, given a shorter exposure than the rest, shows the final state of the crystal.

Fig. 3 is a plot of the increase in area of the crystal shown in fig. 2. measured by weighing cut out prints. The points which correspond to pictures in fig. 2 are lettered. The increase is measured with respect to fig. 2a, as there is no way of knowing what changes occur before this. Extrapolating the curve back to zero dose indicates that the expansion before the first point is 5%. The curve is of the form

$$(\% \text{ increase in area}) = B[1 - \exp(-C \cdot \text{dose})]$$

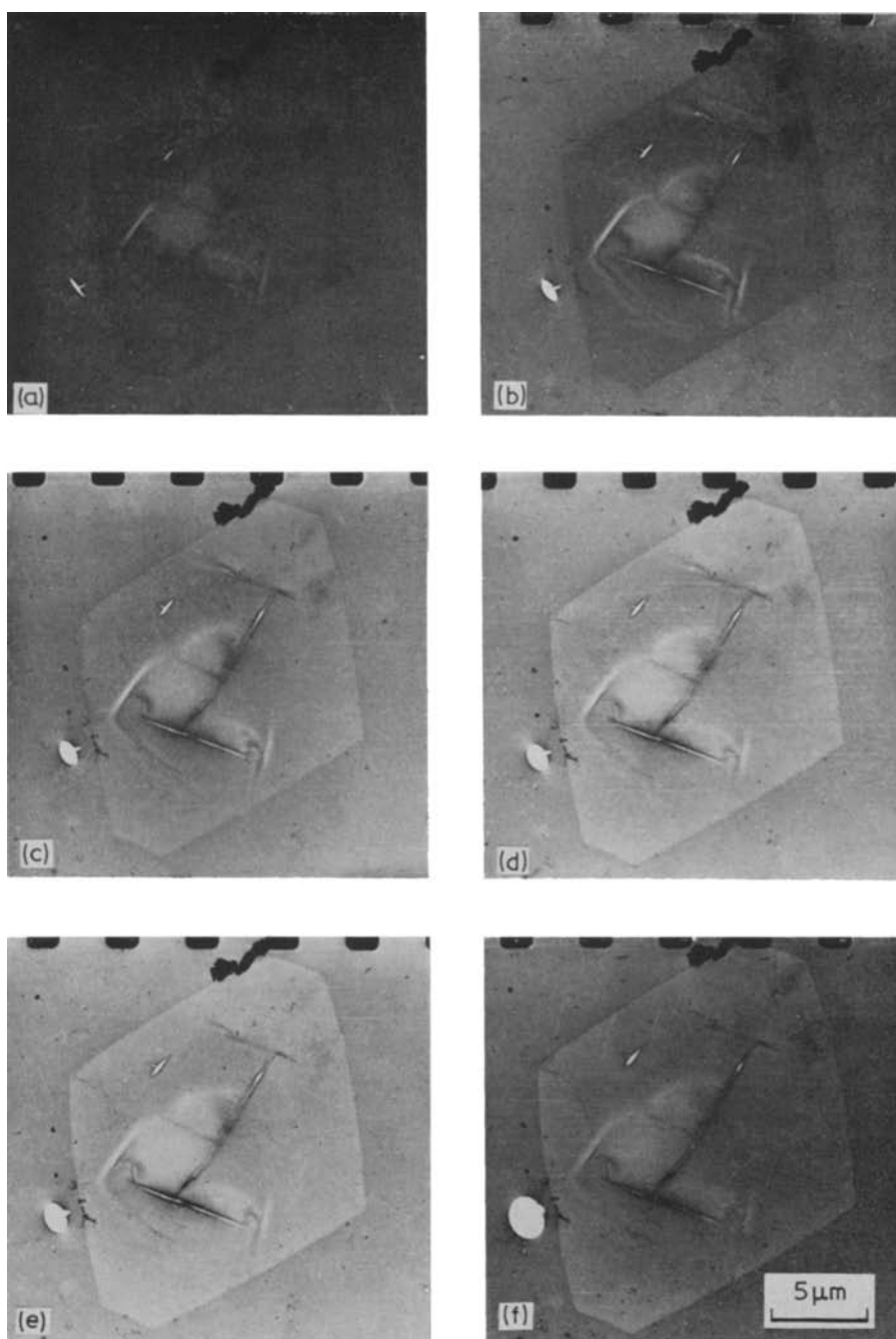


Figure 2 Sequence of electron micrographs of a single crystal of polyethylene mounted on collodion. (a)-(e) Have been processed in the same way, and show the contrast changes correctly. (f) A shorter exposure, shows the final state of the crystal.

The average values of the constants were found to be

$$B = 53 \pm 7\%$$

$$C = 0.009 \pm 0.001 \text{ m}^2/\text{C at } 80 \text{ kV.}$$

Crystals of the same thickness, but made using different types of PE (section 2) did not give significantly different results, but if formvar was used instead of collodion, the final expansion, B ,

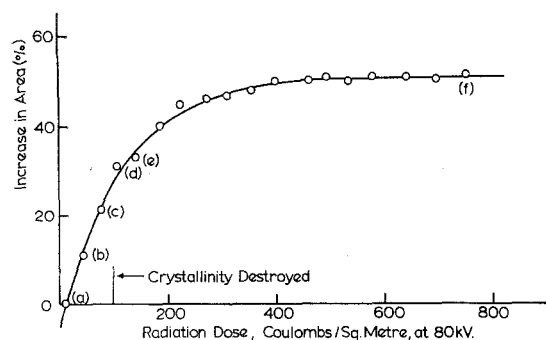


Figure 3 Plot of increase in area versus radiation dose of the crystal shown in fig. 2.

was reduced to $36 \pm 12\%$.

Collodion film containing no PE crystals tends to contract on irradiation in the electron microscope but is constrained by the supporting grid. Thus wrinkles in the film are quickly smoothed out, and any holes or cracks enlarge (as in fig. 2). If the film is flat and continuous, material in the irradiated area contracts, drawing in new material. This contracts in turn, so it takes some time to reach equilibrium. The final contraction of an area well away from a grid bar is typically 15% in area, but it can be prevented entirely if the film is constrained locally. The

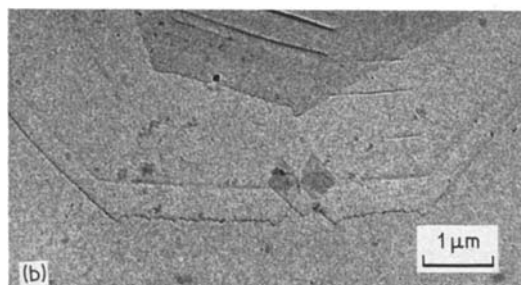
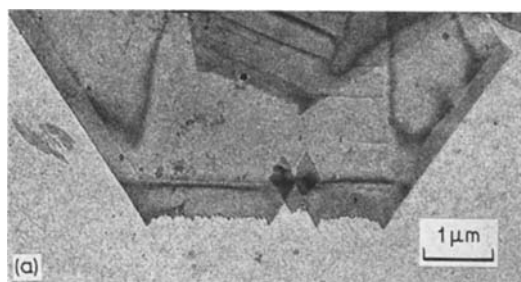


Figure 4 Detail of a group of polyethylene single crystals mounted on collodion, showing greater expansion of superposed layers. (a) Initial state. (b) Final state.

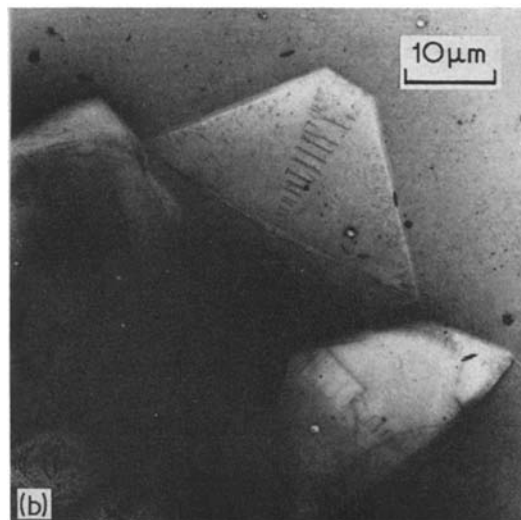
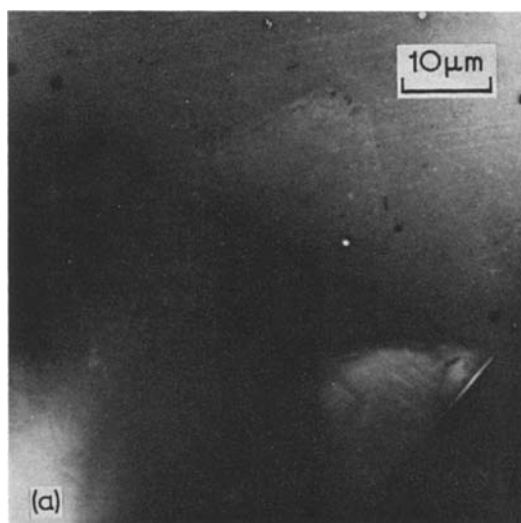


Figure 5 Group of polyethylene single crystals mounted within a thick collodion film. (a) After short exposure to the electron beam. (b) Increased contrast after long exposure.

collodion immediately adjacent to a PE crystal does not change in area by more than a few per cent.

Measurements of expansion in a clump of crystals, or on a multilayer crystal, give quite variable results, but there is always a trend towards greater expansion for thicker crystals. Fig. 4 shows a detail, where a two layer crystal has been overlaid by a third on deposition. The linear expansion across the page is 22% for the first layer, 29% for the second, and 33% for the

third. The expansion at right angles to this is very small.

Fig. 5 shows a clump of crystals mounted within a film of collodion, much thicker than that in figs. 1 and 2. It is difficult to take micrographs at low doses, because the thick film requires higher beam currents for a given image intensity and makes the crystals invisible initially. Only the very thick crystal in the lower left of fig. 5 could be seen on the fluorescent screen at first. Fig. 5a was taken after a dose of about 30 Cm^{-2} at 100 kV. The single layer crystal is visible, but the image is blurred, because the specimen was moving. Fig. 5b was taken after a dose of more than $1,000 \text{ Cm}^{-2}$. The picture is sharp and the contrast has increased; the area containing the crystal appears much lighter, hence thinner than the surrounding collodion. The crystal at the lower right of fig. 5 has collapsed by folding, and is therefore at least two layers thick, but its final appearance is brighter than the single layer crystal. Details in the single layer crystal conform to this pattern: the central pleat parallel to the b axis, a normal collapse feature where the crystal is three layers thick, appears darker than the rest of the crystal in fig. 5a, but brighter – therefore thinner – than the rest in fig. 5b. Further, the narrow border to the crystal, which crystallised on cooling the suspension from the growth temperature, is always thinner than the rest of the crystal. It appears definitely darker – therefore thicker – than the rest in fig. 5b. The wrinkles in the $\{100\}$ sector become very clear in fig. 5b, and it also seems that the sector as a whole is darker than the adjacent $\{110\}$ sectors.

With the help of L. W. Hobbs, of the Department of Metallurgy, Oxford University, specimens were observed in a Siemens Elmiskop I, while being cooled with liquid helium. Fig. 6 shows a PE crystal mounted on collodion, before and after irradiation at 18°K . There is a reversal of contrast, and an increase in area which is on average $25 \pm 10\%$, about half that at room temperature. The other differences are the distorted corners and the thick rim of most of the crystals as in fig. 6b.

3.1.2. Crystals Bridging Holes

Most crystals mounted on the fine grid did not have enough support and merely crumpled and sagged downwards in the beam. Sometimes crystals supported each other without overlapping too much, and fig. 7 shows such a case.

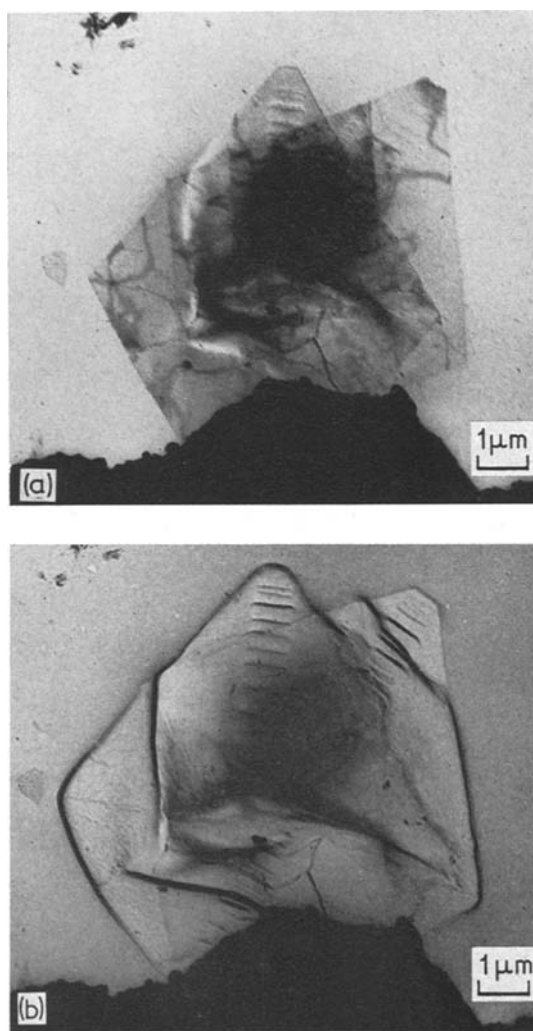


Figure 6 Polyethylene single crystals mounted on a collodion film and observed in the electron microscope at 18°K . (a) Initial state. (b) Final state.

Two multilayer crystals are supported by opposite grid bars and overlap only at their tips. In fig. 7a, taken at very low dose, the regular corrugations of a collapsed $\{100\}$ sector can be seen, as can dark bend contours, which show that the crystals are not yet damaged by radiation. Fig. 7b, shows the same area after a long period of irradiation. There is gross distortion, and the crystals seem to have pushed into each other. The projected area of the crystals has increased by 10%, but because the crystals have become severely buckled the true increase in area must have been greater.

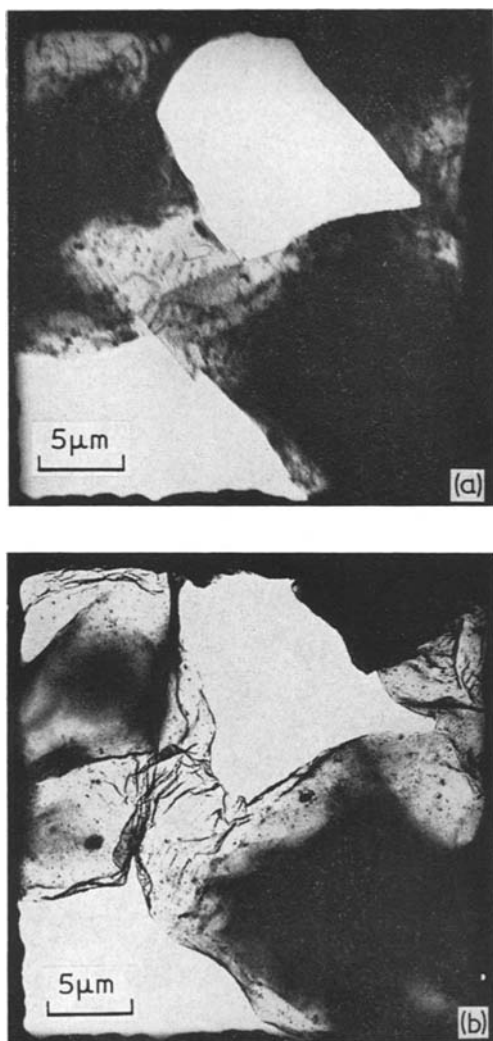


Figure 7 Polyethylene single crystals bridging a hole in a fine mesh grid with no supporting film. (a) Initial state. (b) Final state.

3.2. Thickness Changes of PE Crystals

When crystals which have been irradiated on a collodion film are shadowed with heavy metal, there is no distinct shadow at the edge of the crystal. In any case, with an unstable substrate, an observed step height would not necessarily be the thickness of the crystal. The final thickness could be deduced from the results in the previous section, if the density of the irradiated material was known.

Consider a crystal of area A , thickness t , mass m , and density d . Then $tA = m/d$. After irradiation $t'A' = m'/d'$

If before irradiation $t = A = m = d = 1$, then from section 3.1,

$$A' = 1.53 \text{ and } m' = 0.95 \quad [15]$$

$$\therefore t'd' = 0.95/1.53 = 0.62 \dots \dots \dots (1)$$

The tiny volume of the irradiated samples makes direct density determination impossible, but if crystals irradiated on a carbon substrate have the same final density, d' , it can be found by measuring their thickness after irradiation, t'' . Since the area of crystals irradiated on carbon is held constant, the change in thickness is given by:

$$t''/t = (m'/d') \cdot (d/m) = 0.95d/d'$$

Small areas of a carbon mounted specimen were heavily irradiated, and photographed for later recognition. The specimen was then removed from the microscope and shadowed with gold-palladium alloy at an oblique angle, approximately $\tan^{-1} 0.2$. On returning the specimen to the microscope to measure the shadows cast by the crystals, it was clear that the irradiated areas had buckled, so the shadowing angle was not constant. The distortion was not random, each group of crystals formed a domed bulge so that the shadow length was increased. This confirms that the crystals are trying to expand, but makes measurement more difficult. Local tilts of the specimen affect the projected depth of shadowing metal as well as the projected shadow length. A microdensitometer trace gives, at the same time, the length of the shadow and its depth in terms of photographic density. With this data, and the unaffected shadowing angle, it is possible to calculate the true height of the crystal assuming that the substrate in the shadow has the same slope as the crystal (Appendix 1). Latex spheres were added to the preparation, and measuring the ellipticity of their shadows in unirradiated areas gave the true shadowing angle. After correction, the results were:

$$t = 127 \pm 11 \text{ \AA}, t'' = 119 \pm 18 \text{ \AA}$$

$$t''/t = 0.94 \pm 0.22$$

$$\therefore d' = 1.0 \pm 0.27$$

and from equation (1) $t'/t = 0.6 \pm 0.2$.

This determination is imprecise, and it may be that the final density of the crystal is affected by the carbon film constraint. Ross [16] irradiated low density (0.94) PE in a nuclear reactor and found that the density decreased to 0.90 at 500 Mrads, then increased to 0.99 at 4,000 Mrads. Extrapolation to higher doses, as given in the

electron microscope, indicates that a density of 1.02 will be reached. Energy loss analysis of PE in a special electron microscope [17] indicates a rapid increase of density to about 1.3.

4. Discussion

During irradiation the PE crystals expand, and have nearly constant mass, so the mass thickness must be reduced. This by itself is insufficient to account for the contrast reversal observed in thick films, especially since the mass and thus mass thickness of collodion is falling more rapidly at the same time. If the expanding PE crystal carries along with it the collodion film on which it rests, this collodion will thin by expansion and by mass loss. Local thinning of the whole of the specimen in this way explains how expansion of a crystal only 130Å thick produces a large contrast change in a thick film. It is possible to make quantitative predictions for single layer crystals on this basis.

Assuming that the intensity transmitted by a film of mass thickness *t* is given by

$$I_1 = I_0 \exp(-t/\tau) \tag{2}$$

Then if that film changes its mass thickness to αt

$$I_2 = I_0 \exp(-\alpha t/\tau)$$

and

$$\alpha = \log(I_2/I_0)/\log(I_1/I_0)$$

Measured in this way, a collodion film of original mass thickness *x*, well away from constraints, thins to 0.40*x* as it contracts by about 15% in area. This means a final mass thickness of 0.35*x* for a film irradiated at constant area, in agreement with Brookes [18]. As the photographic plates have a linear response to electrons [19] the change in mass thickness of small regions of constant area near a constraint can be measured with a microdensitometer. This gives the same result, a final mass thickness of 0.36*x*. Where a PE crystal of original mass thickness *a* is mounted on this film, we have an initial mass thickness (*x* + *a*). If there was no expansion, the final mass thickness would be (0.35*x* + *a*), so with an expansion of 53%, it is (0.35*x* + *a*)/1.53. The collodion adjacent to the crystal does not change in area by more than a few per cent, so the contrast of the PE will reverse if 0.35*x* > (0.35*x* + *a*)/1.53, i.e. if *x* > 5.5*a*.

The PE crystals are 130Å thick, and of density 1, so *a* is 13 mg/m² for a single layer. To find the thickness of the films, it was assumed that all the

carbonaceous materials used have the same value of τ in equation (2), the formula for transmitted intensity. PE crystals mounted on evaporated carbon were used as objects of known mass thickness, and under fixed operating conditions, (80 kV, objective aperture 5.10⁻³r) it was found that

$$\tau = 170 \text{ mg/m}^2.$$

On this basis, the film in fig. 1 has a thickness of 113 mg/m², and we have

| | Thickness in mg/m ⁻² | |
|----------------|---------------------------------|---|
| | <i>Before Irradiation</i> | <i>After Irradiation</i> |
| Collodion | <i>x</i> = 113 | 0.35 <i>x</i> = 39.6 |
| Collodion + PE | (<i>x</i> + <i>a</i>) = 126 | (0.35 <i>x</i> + <i>a</i>)/1.53 = 34.3 |

Obtaining the fractional transmitted intensity from equation (2) and using as the definition of contrast, (I₁ - I₂)/(I₁ + I₂), the result on the screen will be

| | Intensity | |
|----------------|---------------------------|--------------------------|
| | <i>Before Irradiation</i> | <i>After Irradiation</i> |
| Collodion | 0.512 | 0.792 |
| Collodion + PE | 0.476 | 0.817 |
| | Contrast | |
| | <i>Before Irradiation</i> | <i>After Irradiation</i> |
| | 3.8% | - 1.5% |

This can be directly compared with microdensitometer traces from the plates, which give

| | Experimental Contrast | |
|--|---------------------------|--------------------------|
| | <i>Before Irradiation</i> | <i>After Irradiation</i> |
| | 5 ± 0.8% | - 1.2 ± 0.5% |

in reasonable agreement with the above.

Fig. 8 is a schematic drawing of the cross-section of the specimen in fig. 1, where it has been arbitrarily assumed that the density of the collodion is 1.3, both before and after irradiation, so that 113 mg/m⁻² is equivalent to a film 870Å thick.

The contrast change of the PE crystal in fig. 1 is explained by its expansion, directly observed. The more complex contrast changes in fig. 5 would be explained by a greater expansion of thicker regions of the crystal. The expansion cannot be measured directly in such a thick specimen, but a greater expansion of thicker regions is observed in thin specimens, fig. 4. The contrast changes produced in the thin specimen are slight, but the same degree of differential expansion would account for the greater trans-

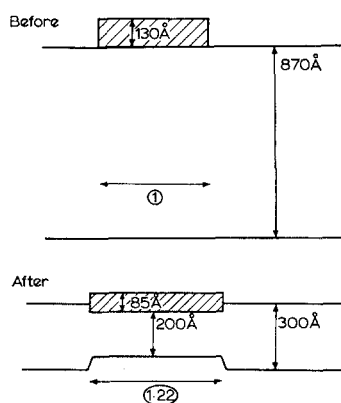


Figure 8 Schematic cross-sectional drawing of the specimen in fig. 1.

parency of multiple layer thicknesses in fig. 5b. Similarly, the lower transparency of the slightly thinner layer edge would follow. Thus observations indicate that greater thickness expands more irrespective of whether the greater thickness is an intrinsic feature of a lamella or whether it has arisen through superposition of layers.

Calculating the final contrast of a single layer crystal in fig. 5 in the same way as above for fig. 1 gives -10% , with the original mass thickness of the collodion estimated to be 370 mg/m^{-2} . The observed contrast in fig. 5b is -5% . In thick films generally the observed contrast is of the right sign, but smaller than expected. We may question the assumption that all the collodion is carried along by the crystal when the collodion is ten or twenty times thicker than the crystal layer, as in this case. Such a thick film may also act as a restraint on the expanding crystal.

The expansion of a lamellar crystal of PE in its own plane on irradiation has been observed under several conditions, and seems a true property of the material. Constraints can reduce the expansion, to less than 0.1% , in the case of a carbon film. (0.1% would cause a $10 \mu\text{m}$ crystal to buckle by 5°). Crystals suspended over holes, which have the least constraint, do not show the largest effect, because they do not remain flat. The advantage of the collodion film, which seems to behave like a viscous liquid during radiation damage, is that the specimen is held flat by surface tension, while motion is allowed in the plane. Viscous forces act against this motion, so the maximum observed expansion of a single layer 130 \AA thick, 22% , may be less than the expansion of a free crystal. The lesser expansion

occurring at 18°K may be an effect of temperature on PE, but the buckled crystal tips, and the pile up of material which has been pushed back indicate that the viscous forces have increased. This is to be expected at low temperature.

The very large deformation may seem strange, since the lamellae are already so thin, and the damage process in PE, cross-linking, brings two chains closer together. However, the molecules in a PE crystal are perfectly oriented along c , except in the fold surfaces, and the end-to-end distance of a single traverse is at its maximum. Therefore any disorder which is introduced must reduce this end-to-end distance. Complete randomisation would give a crystal less than $1/3$ its original thickness, so even with the hindrance of cross-linking, a 40% reduction in thickness is not unreasonable. Unless the process is accompanied by a large increase in density, there must be an expansion in the plane perpendicular to c . The extended length of a chain is proportional to Z , the number of links, and the root mean square maximal projection of a random chain in a given direction is proportional to $Z^{1/2}$. Thus the change in length on randomisation is larger for longer chains, increasing as $Z^{1/2}$, and this would imply a greater expansion. In the case of multiple layers this explanation implies connections between fold stems of consecutive layers. Such connections could be formed by radiation induced cross-links. Preferential cross linking at the crystal surfaces has been indicated previously, e.g. [20-22].

In a collapsed PE crystal, the plane perpendicular to c is not generally the plane of the lamella, but when the crystal is constrained to lie in the plane, as by collodion, a slight tilt makes little difference. If the chain axis is tilted by 30° from the perpendicular, expansion in the plane of the lamella is 10% less along the direction of tilt. This anisotropy is prevented by the continuity of sectors, as the crystal remains planar. The $\{100\}$ sectors can become slightly more transparent, hence thinner than the surrounding crystal. This contrast difference, however, is too small and erratic to be attributed to either different obliquity or different initial thickness.

The irradiation at 18°K showed that the expansion is not a thermal effect, but it is instructive to consider the effect of heat alone on a PE crystal. In general the effect of annealing is to increase the order of a crystal, and on annealing, a PE crystal increases its thickness along c , at the same time reducing its area in the

plane perpendicular to c (e.g. Geil [23], fig. V. 10b p. 321). Here we have radiation, which reduces the order, reducing the thickness along c , and increasing the area perpendicular to c .

The effect reported in this paper and the explanation proposed is not specific to solution grown crystals in polyethylene. It will be seen from the paper to follow that it also accounts for observations on crystals of isotactic polystyrene surrounded by their own amorphous environment. Consequently we may be justified in believing that it will be relevant to the majority of crystalline polymers. Further, even when single crystals are not in isolation but form more complex texture patterns the same processes as described are still expected to pertain to the basic lamellar element of the texture. This should enable predictions to be made about contrast effects when viewing a particular texture. Conversely the generality of the present findings could be put to test by applying the present considerations to account for the puzzling contrast effects reported in certain textures. This has been done in the case of spherulitic films of PE, work that will be the subject of a subsequent publication. At this place it will only be stated that the outcome of the work gives us added confidence that an important clue for the understanding of contrast effects in the electron microscopy of crystalline polymers has been found.

References

1. A. W. AGAR, F. C. FRANK, and A. KELLER, *Phil. Mag.* **4** (1959) 32.
2. A. KELLER, *J. Polymer Sci.* **36** (1959) 369.
3. H. VON ORTH, and E. W. FISCHER, *Makromol. Chem.* **88** (1965) 188.
4. K. KOBAYASHI and K. SAKAOKU, *Lab. Invest.* **14** (1965) 1097.
5. D. T. GRUBB and G. W. GROVES, *Phil. Mag.* (1971) to be published.
6. H. KIHO and P. INGRAM, *Makromol. Chem.* **118** (1968) 45.
7. D. T. GRUBB, 1970, D. Phil. Thesis, Oxford University.
8. J. DLUGOSZ and A. KELLER, *J. Appl. Phys.* **39** (1968) 5776.
9. J. DLUGOSZ, to be published.
10. E. H. ANDREWS, *5th Int. Cong. for Electron Microscopy, Philadelphia* **1** (1962) BB6.
11. P. H. HARRIS (1963) Private Communication.
12. A. KELLER and D. C. BASSETT, *J. Roy. Microsc. Soc.* **79** (1960) 243.
13. D. J. BLUNDELL, A. KELLER, and A. J. KOVACS, *J. Polymer Sci.* **B4** (1966) 481.
14. D. T. GRUBB, *J. Phys. E: Sci. Instrum.* **4** (1971) 222.

15. G. F. BAHR, F. B. JOHNSON, and E. ZEITLER, *Lab. Invest.* **14** (1965) 1115.
16. M. ROSS, AERE Harwell (1954) quoted in A. CHAPIRO, *High Polymers* **15** (1962) 394 (Interscience).
17. R. W. DITCHBURN, D. T. GRUBB, and M. J. WHELAN, paper presented at *Conf. on Electron Energy Analysis*, London, 1971.
18. A. BROCKES, *Z. Physik* **149** (1957) 353.
19. R. C. VALENTINE, in "Advances in Optical and Electron Microscopy", **1** (Academic Press, London, 1966).
20. R. SALOVEY and A. KELLER, *Bell Syst. Tech. J.* **40** (1961) 1397, 1409.
21. R. SALOVEY, *J. Polymer Sci.*, **61** (1962) 463.
22. T. KAWAI, A. KELLER, A. CHARLESBY, and M. G. ORMEROD, *Phil. Mag.* **10** (1964) 107.
23. P. H. GEIL, *Polymer Single Crystals* (Interscience, 1963).

Received 20 July and accepted 10 August 1971.

Appendix

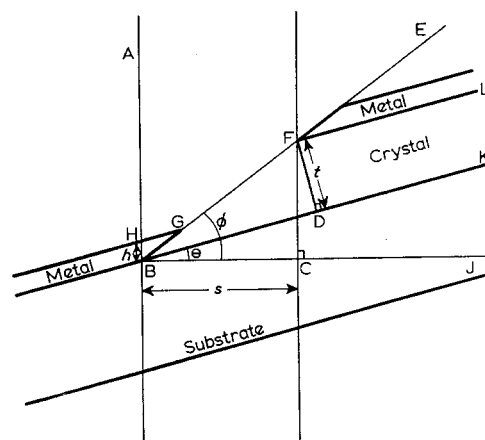


Figure 9 Diagram of specimen which has been shadowed with evaporated metal.

Here the viewing direction is AHB, perpendicular to the mean specimen position BCJ. EFG is the shadowing direction, at angle ϕ to BCJ. The specimen is tilted by θ from its mean position to BDK, so the local shadowing angle, EBK, is $\phi - \theta$. LFDK is a crystal of thickness t , casting a shadow BF. The projected shadow length BC is s , and the projected thickness of the shadowing metal, HB, is h .

$$\begin{aligned} \text{In } \triangle BFD, \sin(\phi - \theta) &= t/BF \\ \text{In } \triangle BCF, \cos \phi &= s/BF \end{aligned}$$

$$\therefore t = s \cdot \frac{\sin(\phi - \theta)}{\cos \phi}$$

In Δ BGH,

$$\frac{\text{BG}}{\sin(90 + \theta)} = \frac{h}{\sin(\phi - \theta)}$$

$$\therefore h = \text{BG} \cdot \frac{\sin(\phi - \theta)}{\cos \theta}$$

If the value of h when $\theta = 0$ is h_{\perp}
then $h_{\perp} = \text{BG} \cdot \sin \phi$

$$\therefore h/h_{\perp} = \frac{\sin(\phi - \theta)}{\cos \theta \sin \phi}$$

$$\therefore t = s \cdot h/h_{\perp} \cdot \tan \phi \cdot \cos \theta$$

The transmitted intensity I is given by

$$I = I_0 \exp[\ln(I_{\perp}/I_0) \cdot h/h_{\perp}]$$

if $I = I_0$ when $h = 0$ and $I = I_{\perp}$ when $h = h_{\perp}$.

$$\therefore h/h_{\perp} = \ln(I/I_0)/\ln(I_{\perp}/I_0)$$

When plates are exposed to electrons, and the optical density D does not approach the saturation density

$$D \propto \text{Exposure} \propto I \text{ (Valentine [19])}$$

Therefore for measurements made on one plate,

$$h/h_{\perp} = \ln(D/D_0)/\ln(D_{\perp}/D_0)$$

$$= \log(D/D_0)/\log(D_{\perp}/D_0)$$

Where D_0 is the optical density of the plate in the region of shadow, D the density outside the

shadow, and D_{\perp} is the density where $\theta = 0$. D_{\perp} is not observable, but can be found if it is assumed that the tilts in unirradiated regions are random, so

$$\bar{\theta} \text{ (no radiation)} = 0$$

$$\bar{I} \text{ (no radiation)} = I_{\perp}$$

The average value of D over different plates must take different exposures into account.

For any plate $D_i = k_i I_i$

$$D_{0i} = k_i I_{0i}$$

But I_0 is the intensity transmitted by the substrate film, which is of constant thickness

$$\therefore I_{0i} = I_0 \cdot (D_2/D_{2_0}) = I_0/I_0$$

and

$$\bar{I}/I_0 = (\overline{D/D_0})$$

$$D_{\perp}/D_0 = I_{\perp}/I_0 = \bar{I} \text{ (no radiation)}/I_0$$

$$\therefore D_{\perp}/D_0 = (\overline{D/D_0}) \text{ (no radiation)}$$

Observed variations in D correspond to $-0.1 < \tan \theta < 0.1$, which means that $\cos \theta \geq 0.995$, and the $\cos \theta$ term can be disregarded

$$\therefore t = s \cdot \frac{\log(D/D_0)}{\log(\overline{D/D_0})} \cdot \tan \phi$$

where $(\overline{D/D_0})$ is the average value from unirradiated regions.